Tidal energy resource characterisation along the French coast by using HF radar and ADCP velocity measurements

Alexei Sentchev, Maxime Thiébaut

Tidal energy resource characterisation along the French coast by using HF radar and ADCP velocity measurements

Alexei Sentchev[#1], Maxime Thiébaut[#2]

[#]*Lab. Oceanography and Geosciences (UMR 8187), Université du Littoral – Côte d'Opale*
32 Av. Foch, 62930 Wimereux, France

[1]alexei.sentchev@univ-littoral.fr

[2]*maxime.thiébaut@univ-littoral.fr*

***Abstract*— A methodology for assessing the tidal flow resource at two sites along the French coast is presented. The first site, located in the Iroise sea (W. Brittany), is selected for demonstration of tidal current conversion technology by Sabella company. The second site - Strait of Dover in the eastern English Channel, has been considered till now as promising. The resource assessment is performed using surface velocity time series recorded by High Frequency radars (HFR) and ADCP velocity measurements in the radar coverage zone. Combination of two sources of data allowed to characterize the current velocity variation in three spatial dimensions and in time which increased confidence in hydrokinetic resource assessment from the radar data. In the Strait of Dover, the most energetic area is found west of Cape Gris Nez, with flow velocities exceeding 1 m/s observed more than 50% of time there. The mean power density attains 0.9 kW/m^2 in the surface layer. In the bottom layer the power decreases by the factor of three. Higher resource is identified at two sites in the Iroise Sea (Fromveur Strait and NW of the Ushant Island) with the mean power density in the surface layer ranging from 2.7 to 3 kW/m^2.**

***Keywords*— Tidal stream resource, HF radar, velocity measurements, Iroise Sea; Strait of Dover**

I. Introduction

Due to the continuous growth of interest for tidal energy conversion by in-stream devices, tidal power industry is in the stage of intensive development. Sites with the biggest tidal stream potential are located on the north-western European shelf [1] and some of them (i.e. Fromveur Strait in the Iroise Sea, Alderney Race or Dover Strait in the English Channel) are considered as very promising for tidal energy projects [1],[2].

Different technologies are operating today at the test sites. In order to optimize the energy conversion, it is required to properly characterize the environmental conditions at sites and thus facilitate the process of selecting tidal power devices appropriate for industrial use. The European Marine Energy Centre (EMEC) has proposed a number of metrics, which helps to evaluate the potential of tidal flow in the most efficient way. The EMEC guidelines include harmonic analysis of velocity time series, turbulence and velocity shear estimation and a comparison between modeling results and in situ measurements [3].

Two approaches can be followed to quantify the tidal stream potential in a most efficient way and to evaluate the major metrics: extensive field measurements and numerical modeling.

The use of a two-dimensional (2D) model to simulate tidal currents is the more convenient and less expensive approach for assessing the hydrokinetic power variability at different space-time scales. Blunden and Bahaj [4] used the TELEMAC-2D modeling system to estimate the available resource at Portland Bill, UK. The model results were used to generate the tidal flow velocity time series over a large area and then to optimize the location of turbine arrays at the site. Xia et al. [5] used a 2D hydrodynamic model to assess the tidal current energy resource in the Severn Estuary, UK. Nowadays, three-dimensional (3D) models are routinely applied for tidal energy site assessment, resource quantification and studies of the impact of energy devices on local circulation and environment. Numerical simulations by Regional Ocean Modeling System (ROMS) were used to examine the tidal asymmetry in a promising site of Orkney Islands [6]. ROMS was also employed for estimating the tidal stream resource variability in the northwest European shelf seas [7].

Remotely sensed velocity observations or in situ velocity measurements at tidal energy sites represent a valuable alternative to modeling. The technique of field data acquisition is well established and currently used for resource characterization in many coastal ocean regions [8],[9]. Acoustic Doppler current profiler (ADCP) is often the instrument of choice for fixed point or towed surveys. In the early studies (e.g. [10],[11]), while the vessel steamed around a circuit, velocity profiles were recorded with sufficient frequency allowing to resolve the vertical structure of the tidal current and its spatial irregularities. More recently, Goddijn-Murphy et al. [8] used underway ADCP data to reconstruct the tidal flow patterns in the Inner Sound (Pentland Firth,UK). Sentchev and Yaremchuk [12] employed the optimal interpolation technique for reconstructing space-time evolution of the velocity field derived from towed ADCP surveys in the Boulogne harbour (English Channel).

But the most frequent are certainly velocity measurements by bottom mounted ADCPs - routinely used for assessing

temporal variations of the tidal stream [12] and turbulent properties of the flow [13]. Turbulent kinetic energy, dissipation rate, Reynolds stress, and some other turbulent parameters can be retrieved from ADCP measurements [14].

In this study, a novel technique of tidal flow resource assessment is presented. It is based on the analysis of surface current velocity time series recorded by High Frequency Radars (HFR) at two energetic tidal sites along the French coast: in the Dover Strait and off the W. Brittany coast. Although the radar technology has been used in many oceanographic applications since more than 20 years (e.g., [15],[16]), its efficiency for large-scale tidal energy resource quantification was demonstrated only recently [17]. At each site, the radar derived surface current velocities were supplemented by velocity profiles acquired by bottom mounted ADCPs in the radar coverage zone. The radars allow continuous acquisition of the surface current velocities over a large area at high spatial and time resolution. ADCP data provide information about velocity variation with depth which is fundamental for detailed tidal stream resource assessment. The knowledge of the three dimensional structure of a tidal flow in combination with the temporal variability of currents allows to assess the resource variability at large scale from direct velocity measurements with a high degree of confidence.

In this way, a detailed characterization of the tidal stream potential was performed in a challenging area - the Strait of Dover, considered as promising for tidal energy conversion. The tidal stream resource was also estimated in a larger area off the W. Brittany coast in the Iroise Sea. One of the highly energetic sites in this area is the Fromveur Strait which is being used since one year as demonstrator for Sabella D10 tidal turbine. The results of our study can be useful for decision makers and stakeholders for future development of renewable energy network at a regional scale.

II. Data and Methods

A. Study Sites and HF Radar Data

In May-June 2003, two Very High Frequency radars (VHFR) were deployed to monitor surface currents off the French Opal coast for a 35-day period. One radar site was located on the Cape Gris Nez (hereafter Cape GN), 40 m above the sea level. The other radar was installed 12 km farther southward, in Wimereux (Fig. 1). The radars, operating at frequencies 45 MHz and 47.8 MHz, measure radial current velocities (projection of current vector onto radar beams) in the surface layer (0.15 m thick) over a distance up to 25 km offshore at high spatial resolution: 600 m along beam and 10° azimuthal spacing, with time resolution of 20 minutes. The radial velocities measured by the two radars were interpolated on a regular grid with 1 km spacing by variational method with gap filling capability. As a result, one month long velocity vector time series were generated from May 1 to June 4, 2003. A detailed description of the experimental settings and methods of data processing of the radar network off the northern Opal coast can be found in [18].

Resource assessment in the Strait of Dover was motivated by a growing interest from both, French and UK sides, to tidal energy conversion by free-stream tidal turbines in this area. The site is shallow water with depth less than 50 m throughout the domain. In the middle of the Strait, there are sandbanks oriented in the alongshore direction (Fig. 1). Sea level has a wide range of variations (4 to 9 m in the French sector), whereas tidal current velocities have a typical magnitude of 1-1.5 m/s [19]. Currents are predominantly semi-diurnal with a pronounced fortnightly modulation due to the interference of the M2, S2 and N2 tidal constituents.

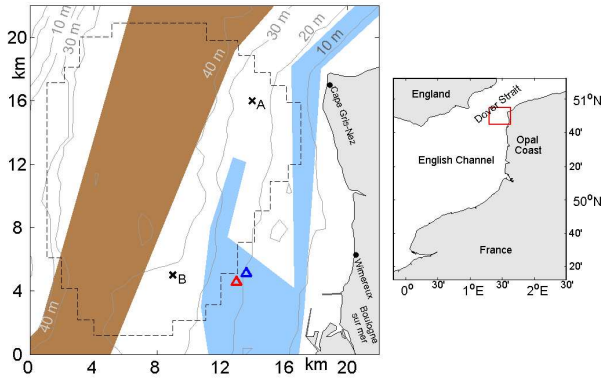

Fig. 1 Study area off the Opal coast in the eastern English Channel (red square on the right panel). Radar sites are shown by black dots and the blue and red triangles denotes the locations of ADCPs in June 2008 and July 2009 respectively. Black crosses show locations A and B selected for a detailed analysis. The navigation way of vessels travelling northward is shown by brown shading. Blue shading matches the main fishing area. Contour interval of the bathymetry is 10 m (grey solid lines). Black dashed line indicates the radar coverage zone. Geographic names used in the text are also shown.

Site assessment should take into account the environmental constraints relative to local economic activities. The Dover Strait is one of the busiest seaways in the world. More than 400 commercial vessels cross the strait daily. The traffic safety is a critical issue because of high risk of collision in the strait. The navigation way of vessels travelling northward is shown by brown shading in Fig. 1. The port of Boulogne is the biggest fishing port in France. Fishing is an important local economic activity and a large area is extensively exploited in the vicinity of the BLH (Fig. 1, blue shading). These constraints considerably limit the area suitable for marine renewable energy conversion.

Two particular locations not affected by constraints mentioned above, are chosen for further detailed analysis of the technically exploitable potential in the study area: northern and southern sectors of the radar coverage zone (Fig. 1). The water depth ranges from 25 to 35 m there, which is favorable for tidal turbine installation [20]

The study site off the western Brittany coast of France has larger extension (Fig. 2). The water depth gradually decreases westward from 50 to 150 m. A group of small islands, islets and rocks form Molène archipelago. There is also a bigger island (8 × 4 km) - Ushant Island, separated from Molène Islands by the 2 km wide and 60 m deep Fromveur Strait. Promising sites for tidal energy production are located around the Ushant Island, representing the second tidal stream potential in France after the region of Alderney Race.

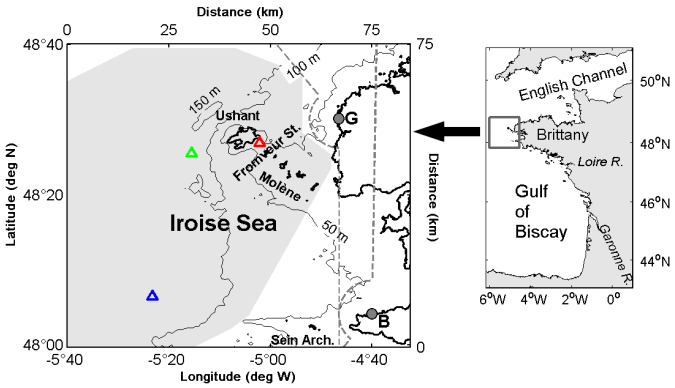

Fig. 2 Study area in the Iroise Sea with radar coverage zone (grey shading), radar sites (grey circles). The red, blue and green triangles denote the locations of ADCPs in the Fromveur Strait, West of Ushant Island and in the southern periphery of the study domain respectively. Contour interval of the bathymetry is 50 m (black solid lines). Geographic names used in the text are also shown.

Two high-frequency Wellen Radars (WERA) operating at 12.4 MHz are deployed on the W. Brittany coast since July 2006. Individual radar sites are located at Cape Garchine (site G), a seashore flat-ground area, and Cape Brezellec (site B), 50 km southward (Fig. 2). In the present study, the radar network was configured to provide velocity estimates at high spatial resolution: 1.5 km along beam and 2° azimuthal spacing, and temporal resolution of 20 minutes. The HF radars measure surface current velocity in a layer of approximately 1 m thick. Radial velocities measured by two radars were interpolated on regular grid of 1 km spacing and combined to form current vectors using 2D variational interpolation technique 2dVar. The accuracy of the radar-derived velocities has been estimated by SHOM (Oceanographic Division of the French Navy) through a comparison with surface drifters and ADCP current measurements for a period of 7 months. In the majority of situations, the discrepancy in velocity measured by different instruments did not exceed 0.15 m/s [21]. In this study, we used velocity time series for the period 04/2007 - 09/2008. A detailed description of the experimental settings, the methods of radar data processing in the Iroise Sea can be found in [18].

B. ADCP Data

ADCP measurements from two 1.2 Mhz upward-looking four-beam broadband RDI ADCPs were used to supplement surface velocities provided by the radars in the Strait of Dover. Both instruments were installed approximately 6 km west of the BLH at 18 m mean depth (Fig. 1). The first ADCP was deployed from 1 to 4 July 2008, during spring tide, and the second one from 9 to 16 June 2009, covering the period of tide evolution from spring to neap. Velocities were recorded at 1 Hz in beam coordinates with 0.5 m vertical resolution, starting from 1 m above the bottom. The data from the surface 3 m thick layer were not considered in analysis because of signal contamination by surface waves.

In the Iroise Sea, ADCP measurements were available in three points within the radar coverage zone: in the Fromveur Strait, west of the Ushant Island and in the southern periphery of the study site (Fig. 2). In these locations, the velocity profiles were recorded by bottom-mounted broadband 600 kHz RDI ADCP.

In the Fromveur Strait, ADCP was deployed during 14 days, from March 19 to April 2, 1993. Velocities were recorded at 0.2 Hz every 4 m, from 6 m to 52 m above the bottom. The deployment depth was 53 m. Given the strength of tidal currents in the Fromveur Strait, in situ data acquisition is very difficult and hazardous. In this sense, the ADCP measurements in 1993 represent the unique data. Thus, they were used for comparison with radar velocity records. A period from September 07, 2007 to September 18, 2007 was selected for the comparison and joint analysis of ADCP and radar data. It is characterized by similar hydrodynamic conditions: secondary spring tide and low wind.

The ADCP located west of the Ushant Island was deployed at 110 m depth from June 16 to July 29, 2006. Velocities were recorded every 3 m starting from 4 m above the bottom. The ADCP velocity profiles for 40-day period (17 June - 27 July 2006) were time averaged within 20 minutes.

The ADCP located in the southern part of the study area was deployed at 120 m depth from June 6 to September 13, 2007. Velocities were recorded every 5 m starting from 8 m above the bottom. The velocity values in the surface 20 m thick layer were removed because of signal contamination by surface waves. The ADCP velocity profiles for 30-day period (17 July - 17 Aug. 2007) were time averaged within 20 minutes and synchronized with the radar acquisition period. This period was characterized by low to moderate wind

C. Data Analysis

Following the guidelines proposed by EMEC [3], the major parameters of tidal flow conventionally used for tidal energy site screening were estimated from the HFR velocity measurements. Current velocity spectrum was also estimated, it can help to explain an interaction between principal tidal constituents resulting in a strong distortion of the tidal velocity curve.

1) Current Strength, Direction and Asymmetry

Current strength characterization involves an assessment of the maximum, time averaged velocity, and also asymmetry of the tidal flow. The mean velocity is the average of current velocity magnitudes over a long period including values around slack water or over specific stages of the tidal cycle such as spring and neap tide.

The maximum sustained velocity represents the maximum current observed. This parameter establishes design loads on device support structures and foundations.

Tidal flow asymmetry concerns, first, the asymmetry of velocity magnitude. An imbalance between the strength of flood and ebb current speeds can exist, generating a considerably more power production during one stage of the tide. To determine the asymmetry a, the following expression was used: $a = \langle V \rangle_{flood} / \langle V \rangle_{ebb}$, where brackets denote time averaging of velocity values on flood and ebb flow respectively, including slack water periods.

Current direction is a principal (dominant) direction of the flow. This is a relevant metric for tidal stream energy conversion as the predominant design concept for a tidal energy converter is that of a fixed horizontal axis turbine. The principal component analysis (PCA) [22] technique was applied to HFR velocity data set in order to determine the principal direction of the flow during the ebb and flood tidal phase. The direction asymmetry $\Delta\theta$ was estimated showing a deviation of the flow from a straight line (dominant direction). That metric is defined as: $\Delta\theta = | \theta_{flood} - \theta_{ebb} - 180° |$ [9]. The standard deviation of current direction for both ebb and flood flow was also established.

2) Hydrokinetic Resources

A simple way to characterize the resource at a site is to estimate the power density available of the flow (per m2 of turbine swept area) for different stages of tide and to describe its spatial distribution. As the HFR measurements are particularly efficient for current monitoring, it is possible to evaluate the available theoretical power P(t) from kinetic energy extraction at different time and space scales using the conventional formula: $P(t)= 0.5\rho V(t)^3$, where ρ is the seawater density, and V(t) is velocity magnitude. To take into account the velocity decrease with depth, a power law relation derived from the best fit of ADCP data was used.

For tidal power projects it is customary to determine the percentage time that a specified current speed is exceeded during a given period of time. In the same way, available power can be analysed. Resulting power and velocity occurrence distribution is also a relevant metric for resource characterization at a site. They provide an indication of time favourable for power generation. For the statistical description of surface current velocities measured by HFR a Weibull distribution was used. This helps to evaluate the importance of velocity ranges for energy production, and also limitations and stresses acting on the energy conversion devices. The cumulative distribution function of current velocity can be approximated by a Weibull function: $F(v)=1 - exp[-(v/\lambda)^k]$, where $\lambda > 0$ is the scale parameter and $k > 0$ is the dimensionless shape parameter [23]. A linear regression method was used to determine these parameters.

3) Velocity Profile

Generally the maximum velocities are observed near the surface and minimum values near the seabed. To determine a beneficial hub-height and optimize the turbine design, the knowledge of velocity profile is required. Tidal current velocity profile throughout the water column is commonly approximated by the power law: $V(z)=V_0\ (z/d)^{1/\alpha}$ [24]. Here, V_0 is the surface velocity, d is the bottom depth, z is the distance above the seabed, and α is an empirical coefficient estimated from linear regression fit of LogLog representation of velocity. This expression allows to account for velocity variation in the boundary layer with reasonable accuracy and in a large depth range as the tidal boundary layer thickness extends to several dozens of meters [25]. When the water depth exceeds hundred meters, V_0 represents a velocity outside the boundary layer (i.e. free stream velocity) which often shows a linear variation with altitude.

III. Results

A. Tidal Stream Resource in the Strait of Dover

1) Current Velocity and Asymmetry from Radar Data

The parameters of synthesized tidal current ellipses used to quantify spatial variability of tidal currents derived from PCA are shown in Fig. 3 for 16 May 2003. During this day, the strongest currents of spring tide were observed. Ellipse orientation shows that the current is strongly controlled by the topography, producing alignment of the major axes along the depth contours. Anisotropy in current field with a relatively high ellipticity is observed over the sandbanks, in the middle of the study domain.

White and black ellipses in Fig. 3 indicate that the current are rotating clockwise (cw) and counter-clockwise (ccw) respectively. Two distinct zones with opposite sign of rotation of the tidal current vector are clearly identified. They are separated by a line roughly following the 30-m isobath. It suggests that, in this location, tidal motion produces alternatively divergence or convergent of surface currents during certain periods of the tidal cycle.

The time averaged current velocity distribution shows low spatial variations with values ranging from 0.5 to 1 m/s, with the highest velocity value observed off the Cape GN. The maximum surface current speed observed by the radars is higher than 2 m/s in the entire study area.

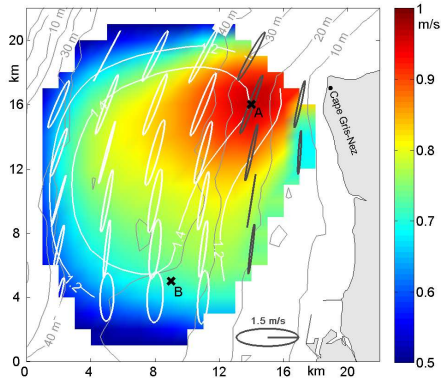

Fig. 3 Mean surface current velocity during the whole study period (color shading) and during the spring tide period in May 2003 (white contours). Shown also tidal current ellipses derived from PCA on May 16, 2003 (every third ellipse is shown). Black ellipses denote counter-clockwise rotating tidal currents and white ellipses denote clockwise rotating currents. Black crosses show locations selected for detailed analysis.

The current asymmetry a is found higher than 1 in almost whole study domain (Fig. 4), indicating the flood flow dominance. The only exception is the eastern part of the area where the asymmetry is slightly less than 1. The maximum current asymmetry (a = 1.6) is observed 6 km westward of the Cape GN, indicating the effect of cape on spatial distribution of phase and amplitude of the principal (M_2) tidal constituent and its higher order harmonics (M_4, MS_4) [26]. A strong imbalance between the strength of flood and ebb current

speeds can cause much larger asymmetry in power extraction thus reducing the overall energy yield.

Current direction is another relevant metric for tidal stream energy conversion as the predominant design concept for energy converter is that of a fixed horizontal axis turbine. In the Dover Strait, the asymmetry $\Delta\theta$ between the principal direction of ebb and flood flows varies from 2° to 10°. The minimum asymmetry is observed in the southern part of the domain. $\Delta\theta$ gradually increases until 10° in the northern part, where the maximum current occurs.

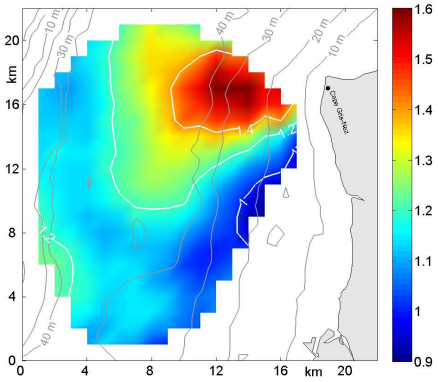

Fig. 4 Current velocity asymmetry *a* distribution.

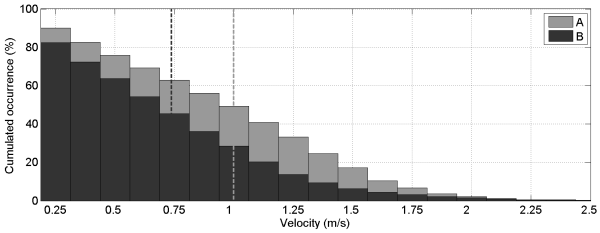

Fig. 5 Cumulative occurrence of velocity magnitude in locations A and B (see Fig. 1 for location). Dashed lines represent the mean velocity values.

In tidal energy projects, it is customary to estimate the occurrence of different velocity values observed during a given period. Velocity histograms provide a simple way to evaluate the available resource at any point of a site. They indicate what percentage of time could be used for power generation. Fig. 5 shows the cumulated occurrence of tidal current velocity observed in two locations selected for detailed analysis: point *A* located westward of the Cape GN and point *B* located westward of the BLH (see Fig. 1 for locations). The strongest currents are observed in *A*, whereas *B* is located not far from the ADCP deployments.

The velocity of 1 m/s is exceeded 50 % of time in location *A* and 25 % of time in location *B*. The current speed of 1.5 m/s is exceeded 3 times more often in *A* than in *B* (respectively 18 % and 6 % of time). The mean current velocity is found to be 1 m/s in *A* and 0.75 m/s in *B*. This difference results from the change in flow regime. The strait narrowing and the presence of Cape GN cause flow acceleration and provides the highest tidal current velocity there.

2) Velocity Profiles

Velocity profiles from bottom mounted ADCP off the BLH were analyzed for different stages of the tidal cycle: peak velocity period (PV), flood and ebb flow period preceding and following the peak velocity. The time interval used for analysis was set to one hour for each tidal stage. The velocity profiles recorded during multiple 1-hour intervals were considered for each of the three tidal stages encountering the peak velocity. Fig. 6 shows the time averaged velocity profiles observed during flood and ebb tidal flow. Based on the data acquired in 2008 and 2009, the vertical profile was found following the $1/6^{th}$ law on flood tide and the $1/7^{th}$ law on ebb tide. The analysis also shows that lower value of α is achieved one hour before the peak velocity. Then, it gradually increases until the maximum value, reached one hour after the peak velocity (Table 1). Moreover, α shows larger variation on ebb tide than on flood tide with values ranging from 6 to 7.5 and 5.5 to 6.5 respectively (Table 1). The mean error of α estimation (standard deviation Δα) for each 1 hour long period of tidal flow was found close to 1.

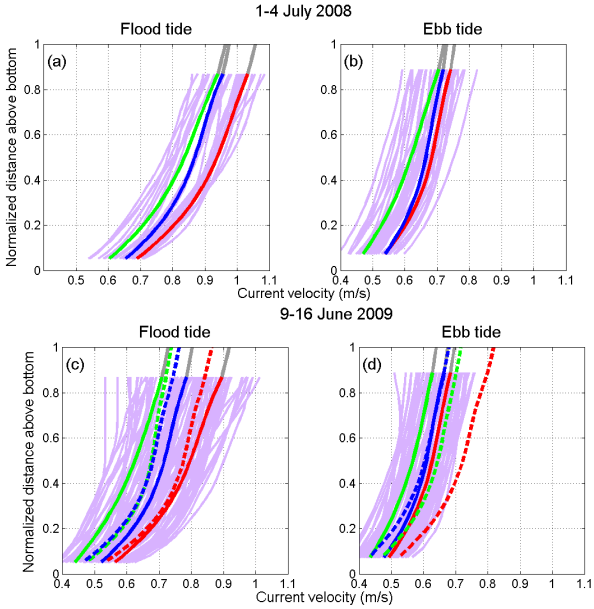

Fig. 6 Current velocity profiles during flood and ebb tide flow derived from ADCP measurements in 2008 (a) and in 2009 (b). Mean velocity profiles during the peak current are shown in red (one hour averaging period is centered on peak velocity). One hour averaged velocity profiles observed one hour before and one hour after the peak velocity are given in green and blue respectively. Velocity profiles provided by ADCP (20-min averaged) are given in mauve. Only profiles with depth averaged velocity > 1 m/s i(a,b) and > 0.5 m/s (c,d) are shown. Colour solid and dashed lines match observed and modeled velocity profiles. Profile extrapolation to surface is shown in grey.

Following the same methodology, velocity profiles from a regional, extensively validated numerical model [27] were analyzed and compared with profiles from ADCP measurements in June 2009. The model simulates velocity distribution in the whole water column, including the surface layer. There, ADCP does not provide reliable velocity measurements. Only extrapolation allows approximating the velocity distribution in the uppermost surface layer. Fig. 6cd shows high degree of consistency between velocity profiles obtained from the model and from the ADCP measurements.

Power law parameter α is in a very good agreement for modeled and observed profiles with relative error not exceeding 7%. The shape of velocity profiles generated by the model for different stage of tidal cycle shows low variation with the standard deviation Δα = 0.3 on average (Table 1).

TABLE I
POWER COEFFICIENT α OF THE VELOCITY PROFILES APPROXIMATED BY A POWER LAW FOR THREE SPECIFIC PERIODS OF TIDAL FLOW EVOLUTION AROUND THE PEAK VELOCITY (PV), FOR FLOOD AND EBB TIDE

		PV-1h	**PV**	**PV+1h**	**< α >**	**Δα**
Flood	ADCP	5.6	6.1	6.5	6	1.1
	MODEL	5.6	6.2	6.7	6.1	0.3
Ebb	ADCP	6.0	7.1	7.5	6.9	1
	MODEL	6.2	7.4	7.6	7	0.2

Histograms of cumulative occurrence of velocity magnitude derived from the model and from observations (not shown) revealed that the model velocities are slightly overestimated (by 5%) with the exception of very low velocities (< 0.35 m/s). For this range, the modeled velocities are lower than observed velocities.

3) Tidal Stream Potential

The kinetic power density is the primary metric used to characterize the theoretical potential and its variation at a site. The radar observations provide information about spatial and temporal variability of surface currents. It is also assumed that the ADCP derived velocity profiles are representative for ebb and flood flow at each grid point within the study domain. By merging these two sources of data, it is possible to estimate the available power density at different space and time scales and at vertical levels directly from velocity observations. Most of the tidal turbines are designed for deployment on the sea floor (e.g. Open Hydro, Sabella) but some of them (e.g. Hydro-Gen, Evopod by Oceanflow) are installed in the surface layer to take advantage of the highest current velocities. For this reason, the power density should be estimated for different altitudes according to device's deployment level.

Combining ADCP derived profiles and HF radar surface velocity measurements available during one month period, the power density time series in the surface and bottom layers (upper and lower half of the water column) were generated and then time averaged. In this calculation, it was assumed that the vertical variation of the current velocity follows the $1/6^{th}$ and the $1/7^{th}$ power law on flood and ebb flow respectively.

As the only variable parameter governing the power is the current velocity, it is not surprising to find similar spatial patterns for both mean tidal current velocity and mean kinetic power density distribution (not shown). In the surface layer, the mean power density attains its maximum value (0.9 kW/m²) in the northeastern sector – west of Cape GN, with peak value of 5 kW/m². For the rest of the study domain, the mean available power is much lower and varies in the range 0.1 - 0.6 kW/m². In the bottom layer, the maximum value of the mean power (0.3 kW/m²) is also found west of Cape GN. On average, the kinetic power available in the bottom layer is 3 times lower than that available in the surface layer. During spring tide, the power in the tidal flow increases considerably and attains 2.2 kW/m² and 0.7 kW/m² in the surface and bottom layers respectively, in the northeastern sector.

Fig. 7 represents time series of hourly and daily mean power density estimates for two geographic locations selected above: west of Cape GN (A) and west of Boulogne (B) (see Fig. 1 for location). At time scale of a day (Fig. 7a), a semi-diurnal variability and a pronounced inequality of kinetic power are observed in the surface and bottom layers. The latter is caused by current asymmetry – stronger in location A (a = 1.6) than in location B (a = 1.1). Peak power during flood tide in location A and B, is respectively 3 and 2 times higher than that during ebb tide. For a month long period, a fortnight modulation of power is observed (Fig .7b). On average, the mean power available in location A exceeds that in location B by a factor of two.

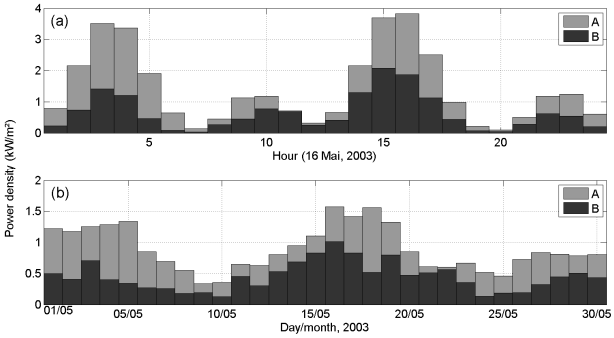

Fig. 7 Hourly (a) and daily (b) values of power density in the surface layer in location A (grey) and B (black).

B. Tidal Stream Resource in the Iroise Sea

Using the same approach of data analysis (year long velocity time series were analysed), we summarize hereafter the main features of tidal flow and resource variability in the Iroise Sea, with emphasis put on the region around the Ushant Island.

1) Current Velocity and Asymmetry

Spatial and temporal variability of tidal currents are quantified by estimating the parameters of synthesized tidal current ellipses derived from the principal component analysis (PCA) of 4-day long spring tide velocity time series. The length of ellipse's semi-axis provides information about the tidal current strength and indicates regions with the most powerful flow (Fig. 8). The maximum and time averaged current velocity distribution shows significant spatial variations and ranges from 0.75 to 4 m/s for the maximum velocity (Fig. 8 colour shading) and from 0.5 to 2 m/s for the mean spring tide velocity (Fig. 8 black contours).The strongest current are identified in two areas: west of the

Ushant Island and in the Fromveur Strait. Bathymetry gradients and the presence of islands cause flow acceleration, tend to tighten the streamlines and provide the maximum velocities there. In these two sectors, the mean velocity exceeds 1.5 m/s and the maximum attains 4 m/s.

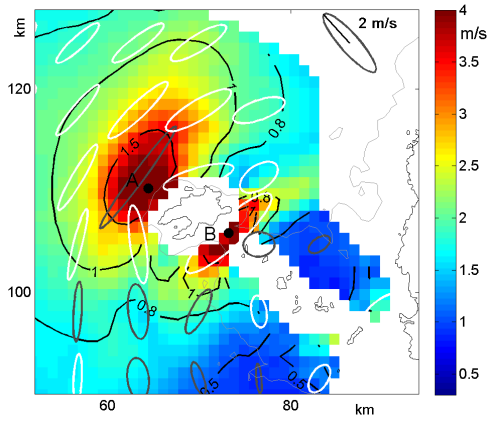

Fig. 8 Tidal current ellipses during spring tide. Every sixth ellipse is shown. Black ellipses denote counter-clockwise rotating tidal currents and white ellipses denote clockwise rotating currents. The maximum surface velocity during the study period (color shading) and spring tide average velocity (black contours). Letters A and B mark location of grid points where the highest velocities are observed

The orientation of the principal current clearly shows that the tidal wave arrives from the Gulf of Biscay and travels northeastward toward the English Channel. In the majority of the domain, the tidal current direction is parallel to bathymetry contours indicating that the bathymetry guides the flow. However, in the eastern and southern sectors of the Ushant Island, a significant misalignment in current direction during flood and ebb tide is observed. Such a deviation of the flow during both tidal phases is known as direction asymmetry. It creates difficulties for turbine models designed for bi-directional tides.

Distribution of $\Delta\theta$ within the study area reveals high values (up to 90°). The highest misalignment of tidal currents is observed along the southern extremity of the island. Sentchev et al. [18] documented the presence of transient eddies in these areas which might explain such a large difference in the direction of the dominant current between ebb and flood flow. In the north-western sector of the domain, $\Delta\theta$ ranges from 0° to 10°, indicating that ebb and flood flows are mostly aligned.

Although ellipse orientation, current strength and polarization are similar in the NW of the Ushant Island and in the Fromveur Strait, a noticeable difference between these two areas was documented for the current velocity asymmetry *a*.

The asymmetry varies in a wide range, from 0.5 to 2.5, and shows spatial pattern with $a > 1$ in the west and $a < 1$ in the South (Fig. 9). The strongest variation of asymmetry is observed in the Fromveur Strait. Here, the asymmetry values reach 2.5 in the onshore (north-eastern) sector, indicating that flood flow velocities are by far higher than ebb flow velocities. The asymmetry decreases toward the centre of the Strait, where the tidal flow reaches a balance ($a = 1$). However, another distortion of velocity curve appears seaward, on the exit of the Strait. Here, and within an extended zone south of the Ushant Island, the asymmetry values decrease to 0.5 (Fig. 9) indicating that the flow regime is ebb dominated.

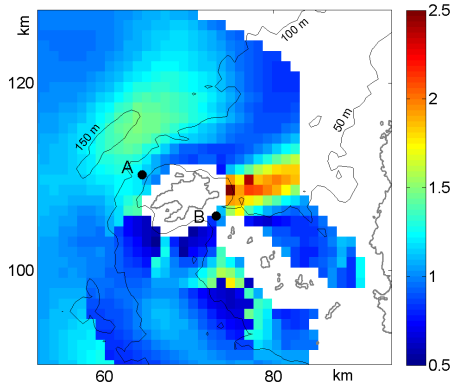

Fig. 9 Spatial distribution of current velocity asymmetry α.

Fig. 10 shows the probability density and cumulated occurrence of tidal current velocity in two grid points where the highest potential is expected (locations A and B in Fig. 8).

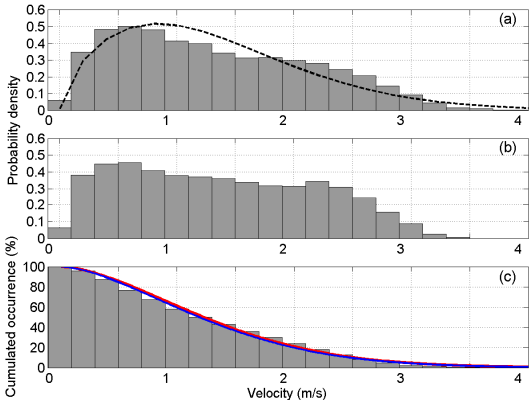

Fig. 10 Probability density in location A (a) and location B (b), and cumulated occurrence of velocity values in A (c). Weibull distribution for cumulated occurrence of velocity is shown by colour lines for A and B. Shape and scale parameters (k and λ) of Weibull law are given in the text. Dashed line in (a) represents Weibull approximation of velocity probability density.

In point A, the probability density roughly follows the Weibull distribution with maximum probability (50%) achieved for the velocity of 0.6 m/s, and then gradually decreases in the range from 1 to 4 m/s (Fig. 10a). In the Fromveur Strait (point B), the probability density looks different (Fig. 10b). The maximum probability is lower (45%) for the same velocity value (0.6 m/s). A clear bi-modal distribution cannot be identified, but the distribution flattening within the velocity range between 0.6 and 2.5 m/s, is observed. Cumulated occurrence distribution (Fig. 10c) is nearly the same in both locations. It perfectly reproduced by the Weibull law with the same scale parameter $\lambda = 1.5$ in each location and a shape parameter $k = 1.6$ and 1.7 in locations A and B respectively.

2) *Velocity Profiles*

The ADCP data collected in the Fromveur Strait were 20-min averaged and then combined together within different periods (one hour long) of the tidal cycle: peak velocity period and periods either side of peak velocity. The resulted time-average profiles were considered and their shape was approximated by a power low for the spring/neap and ebb/flood stages of the tidal cycle (Fig. 11). The results presented here concern the data acquired in the Fromveur Strait. ADCP measurements available in two other locations within the radar coverage zone were processed in similar way and the results occurred not very different. The velocity profiles were found following the power law with $\alpha = 7.5$ on average. Very low variations of the power coefficient α between the different tidal stages are identified. The highest value is reached when the peak current occurs (Table 2).

Time series of the depth averaged velocity derived from ADCP and surface velocities provided by the radars in the nearest grid point were compared. The comparison shows a good overall agreement with zero phase lag, high degree of correlation (0.82), and revealed that the radars overestimate the depth average velocity by approximately 20%.

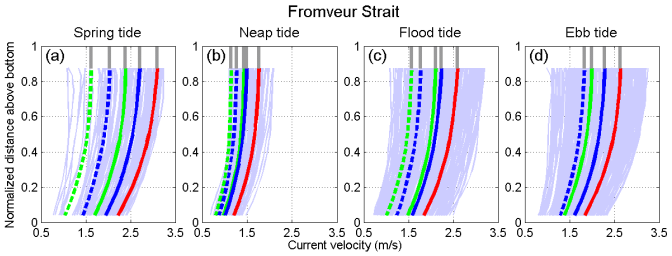

Fig. 11 Current velocity profiles from ADCP measurements in the Fromveur Strait during spring/neap tide (a,b) and flood/ebb tide (c,d). Mean velocity profiles during the peak current are shown in red. One hour averaged profiles either side of peak velocity are given in green/blue solid lines for peak-1h/+1h respectively. Modelled profiles are shown by dashed line. 20-min averaged velocity profiles provided by ADCP are given in purple. Profile extrapolation to surface is shown in grey.

3) *Tidal Stream Potential*

Using velocity time series provided by the radars, the power law expression for velocity profiles derived from moored ADCP data, and the layer extension, the power density time series in the surface and bottom layers were generated and then averaged at different scales.

Hourly mean and daily mean time series of kinetic power density for two locations (A and B) around the Ushant Island are shown in Fig. 12. Strong variability is observed both at daily and monthly scales. For hourly average power time series (Fig. 12ac), a quarter-diurnal variability is clearly seen with peak power density occurring every six hours. A semi-diurnal inequality is also observed. It is more pronounced for location A (NW Ushant) and caused by tidal flow asymmetry there. In the centre of the Fromveur Strait, daily distribution of power density show more regular cycle. The current asymmetry in B is close to 1. Very strong fortnightly modulation of power density is revealed in both locations.

The overall mean values of power density are sensibly the same in both locations and attain 2.7 kW/m^2 in the surface layer. In the bottom layer (15 m thick) the power density is close to 1 kW/m^2. During spring tide, the power density was found higher NW of the Ushant Island (4.8 kW/m^2) compared to the corresponding value in the Fromveur Strait (3.7 kW/m^2).

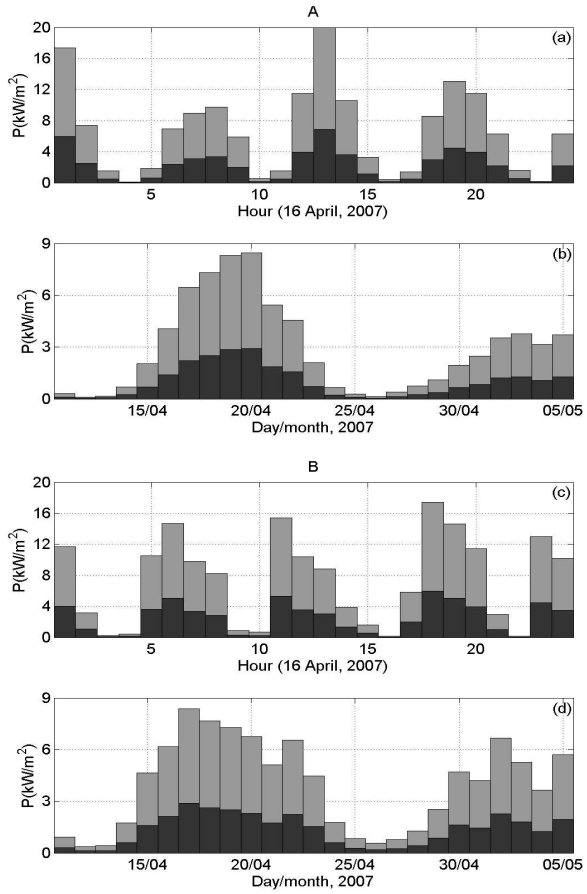

Fig. 12 Time series of hourly mean (a,c) and daily mean (b,d) power density in locations A and B, in the surface (grey) and bottom (black) layer.

TABLE III
POWER COEFFICIENT α OF THE VELOCITY PROFILES APPROXIMATED BY A POWER LAW FOR THREE SPECIFIC PERIODS OF TIDAL FLOW EVOLUTION AROUND THE PEAK VELOCITY (PV), FOR FLOOD AND EBB, NEAP AND SPRING TIDE IN THE FROMVEUR STRAIT

	PV-1h	**PV**	**PV+1h**	**< α >**
Flood	7.6	7.8	7.7	7.7
Ebb	7.3	7.3	7.5	7.5
Spring	7.7	7.9	7.8	7.8
Neap	7.0	7.0	7.3	7.1

IV. Discussion and Conclusions

Assessment of the available tidal stream resource is an essential first step toward successful site selection, device deployment, and further exploitation of the resource [4]. However site selection is not simply a case of identifying regions with large tidal currents. Instead, resource assessment and site selection should consider a wide range of factors, including temporal and spatial variability of the resource and tidal flow parameters, such as current asymmetry, change in phase, velocity profile, … (e.g. [6]). Detailed observational campaigns are not sufficient (or too much expensive) at the scale required for detailed resource characterisation. Therefore, tidal-stream resource assessments typically make extensive use of validated hydrodynamic models (e.g. [28]).

In our study, we present a novel approach for resource assessment based on observations of tidal flow dynamics by oceanographic radars in combination with ADCP measurements. The method can be applied separately or in conjunction with numerical modelling for analysis of tidal stream potential at different sites. It was recently used for resource quantification at a highly energetic site in the Iroise Sea [17], where the French turbine Sabella D10 is deployed since 2015. And it is extended to tidal flow resource assessment in the Dover Strait, which has been considered as promising site.

Using the advantages of radar technology (spatial coverage, high resolution, continuous data acquisition, …) the remotely sensed velocities are used to make large scale quantification of tidal stream resource, of the major metrics of tidal flow and their space and time variation. A significant failure of ADCP point measurements is their inability to provide context of the complex spatial variability of tidal currents that are so often a feature of potential marine renewable energy sites. The use of underway ADCP measurements for tidal energy site screening, an approach developed recently in [8],[12], has also many limitations. The presented novel technique of site assessment enables to avoid this weakness.

Two sites located along the French coast of La Manche (the Iroise Sea is not far from the entrance to La Manche), considered in this study, have benefit from HF radar velocity measurements at different periods. Both sites are considered as promising for marine renewable energy conversion. At both sites, the HF radar observations revealed a large spatial and temporal variability of tidal stream and power density, an important asymmetry of tidal currents which can cause a large imbalance of power production during ebb and flood flow. High current velocity asymmetry as was discovered and mapped around the Ushant Island, to the best of our knowledge, has never been documented before.

The vertical profile of power density was reconstructed and used for quantifying the amount of power available in the bottom and surface layers at different time and space scales. The data analysis showed that the most energetic area in the Dover Strait is located west of the Cape Gris Nez, outside the northward navigation way and fishing area. Velocities exceeding 1 m/s are observed more than 50% of time there and the spring tide velocity is of the order of 1.4 m/s. This provides the temporal mean power density of 0.9 kW/m² in the surface layer and 0.3 kW/m² in the bottom layer. The level of energy available in the flow is assumed sufficient for potential future technology testing in this area.

The analysis of HF radar data in the Iroise Sea revealed two areas with high energy potential and thus more suitable for tidal stream device deployment: the Fromveur Strait and the area NW of the Ushant Island. The maximum current velocity attains 4 m/s there, and the velocity of 1 m/s is exceeded 60% of time at both sites. The mean spring tide current velocity observed in the surface layer attains 1.6 m/s and 1.7 m/s respectively. The map of maximum and mean velocity (Fig. 8) indicates that spatial extension of the former area is much bigger, while the area in the Fromveur Strait with extremely high velocity values does not exceed 6 x 2 km.

The hydrokinetic resources at both sites around the Ushant Island were estimated in the surface and bottom layers. NW of the Ushant Island and in the Fromveur Strait, the estimated annual mean kinetic power density in the surface layer is of the order of 2.7 kW/m². The power available in the bottom layer is 3 times lower. Considerable resource variability on hourly and daily time-scale has been diagnosed. A strong variation of current asymmetry occurring at short distance in the Fromver Strait enables to provide a balanced power generation there by aggregating marine turbines in space.

Acknowledgment

The study was supported by the project PRO-TIDE of the Interreg IVB NW Europe program and represents a contribution to this project. The authors acknowledge funding support by the Pôle Metropolitain de la Côte d'Opale. ADCP data were provided by the Oceanographic Centre of the French Navy (SHOM). The HFR data were provided by ACTIMAR Company with the authorisation of (SHOM). The authors thank Philippe Forget, Yves Barbin (MIO, Toulon) and Max Yaremchuk (NRL, Stennis Space Centre) for their contribution to radar data processing.

References

[1] Commission of the European Communities, *The Exploitation of Tidal and Marine Currents: Wave Energy: Project Results.* European Commission,1996

[2] UK Department, Trade and Industry, "Atlas of UK Marine Renewable Energy Resources: Technical report." 2004

[3] C. Legrand, "Assessment of Tidal Energy Resource: Marine Renewable Energy Guides," The European Marine Energy Center, London, Tech. Rep., 2009

[4] L.S. Blunden and A.S. Bahaj, "*Tidal energy resource assessment for tidal stream generators," Proceedings of the Institution of Mechanical Engineers, Part A: Journal of Power and Energy*, vol. 221, no. 2, pp. 137-146, 2007.

[5] J. Xia, R. Falconer, and B. Lin, "*Numerical model assessment of tidal steam energy resources in the Severn Estuary, UK," Proceedings*

Institution of Mechanical Engineers, Part A: Journal of Power and Energy, vol. 224, no.7, pp. 969-983, 2010.

[6] S.P. Neill, M.R. Hashemi, and M.J. Lewis, "The role of tidal asymmetry in characterizing the tidal energy resource of Orkney," *Renewable Energy*, vol. 68, pp. 337-350, 2014.

[7] P.E. Robins, S.P. Neill, M.J. Lewis, and S.L. Ward, "Characterising the spatial and temporal variability of the tidal-stream energy resource over the northwest European shelf seas," *Applied Energy*, vol. 147, pp. 510-522, Jun. 2015.

[8] L. Goddijn-Murphy, D.K. Woolf, and M.C. Easton, "Current patterns in the inner sound (Pentland Firth) from underway ADCP data", *Journal of Atmospheric and Oceanic Technology*, vol. 30, no 1, pp. 96-111, 2013.

[9] S. Gooch, J. Thomson, B. Polagye, and D. Meggitt, "Site characterization for tidal power", IEEE, 2009, pp 1-10.

[10] W. R. Geyer and R. Signell, "Measurements of tidal flow around a headland with a shipboard acoustic Doppler current profiler", Journal o99f Geophysical Research: Oceans (1978-2012), vol. 95, no. C3, pp. 3189-3197, 1990.

[11] R. Vennell, "Acoustic Doppler current profiler measurements of tidal phase and amplitude in Cook Strait, New Zealand," *Continental Shelf Research*, vol. 14, no. 4, pp. 353-364, 1994.

[12] A. Sentchev and M. Yaremchuk, "Monitoring tidal currents with a towed ADCP system", *Ocean Dynamics*, vol.66, no. 1,pp. 119-132, Jan. 2016.

[13] E. Osalusi, J.Side, and R.Harris, "Structure of turbulent flow in EMEC's tidal energy test site", *International Communications in Heat and Mass Transfer*, vol. 36, no. 5, pp. 422-431, 2009.

[14] J. Thomson, B. Polagye, V. Durgesh, and M.C. Richmond, "Measurements of turbulence at two tidal energy sites in Puget Sound, WA", *Oceanic Engineering*, IEEE Journal of Oceanic Enginnering, vol. 37, no. 3, pp. 363-374, 2012.

[15] D. Prandle, "A new view of near-shore dynamics based on observations of ocean surface currents", Progress in oceanography, vol.27, no.3, pp. 403-438, 1991.

[16] J.D. Paduan and L. Washburn, "High-frequency radar observations of ocean surface currents", *Annual review of marine science*, vol. 5, pp. 115-136, 2013.

[17] M. Thiébaut and A. Sentchev, "Estimation of Tidal Stream Potential in the Iroise Sea from Velocity Observations by High Frequency Radars", *Energy Procedia*, vol. 76, pp. 17-26, 2015.

[18] A. Sentchev, P. Forget, Y. Barbin, and M. Yaremchuk, "Surface circulation in the Iroise Sea (W. Brittany) from high resolution HF radar mapping", *Journal of Marine Systems*, vol. 109, pp. S153-S168, 2011.

[19] A. Ouahsine, H. Smaoui, and A. Sentchev, "Modelling of Tide and Tidally Induced Hydro-Sedimentary Processes in the Eastern Part of the English Channel", *Journal of Marine Environmental Engineering*, vol. 8, no.4, 2006.

[20] S.J. Couch and I. Bryden, "Tidal current energy extraction: Hydrodynamic resource characteristics", *Proceedings of the Institution of Mechanical Engineers, Part M: Journal of Engineering for the Maritime Environment*, vol. 220, no. 4, pp. 185-194, 2006.

[21] A. Le Boyer, G. Cambon, N. Daniault, S. Herbette, B. Le Cann, L. Mariè, and P. Morin, "Observation of the Ushant tidal front in September 2007", *Continental Shelf Research*, vol. 29, no. 8, pp. 1026-1037, 2009.

[22] R.E. Thomson and W.J. Emery, *Data analysis methods in physical oceanography*. Elsevier, 2001.

[23] J.V. Seguro and T.W. Lambert,"Modern estimation of the parameters of the Weibull wind speed distribution for wind energy analysis", *Journal of Wind Engineering and Industrial Aerodynamics*, vol. 85, no. 1, pp. 75-84, 2000.

[24] E.W. Peterson and J.P. Hennessey Jr, "On the use of power laws for estimates of wind power potential", *Journal of Applied Meteorology*, vol. 17, no. 3, pp. 390-394, 1978.

[25] R. Souslby, *Dynamics of Marine Sands: A Manual for Practical Applications*. London: Telford, 1997.

[26] D. Prandle, "Year-long measurements of flow-through the dover strait by HF radar and acoustic Doppler current profiler (ADCP)", *Oceanologica Acta*, vol. 16, no. 5-6, pp. 457-468, 1993.

[27] N. Jouanneau, A. Sentchev, and F. Dumas, "Numerical modeling of circulation and dispersion processes in Boulogne-sur-Mer harbor (Eastern English Channel): sensitivity to physical forcing and harbor design", *Ocean Dynamics*, vol. 63, no. 11-12, pp 1321-1340, Dec. 2013.

[28] M. Lewis, S.P. Neill, P.E. Robins, M.R. Hashemi, Resource assessment for future generations of tidal-stream energy arrays, Energy 83 (2015) 403-415.